Int J Adv Manuf Technol (2014) 71:675–683
DOI 10.1007/s00170-013-5527-3

ORIGINAL ARTICLE

Airfoil profile reconstruction under the uncertainty of inspection data points

Farbod Khameneifar · Hsi-Yung Feng

Received: 23 May 2013 / Accepted: 24 November 2013 / Published online: 6 December 2013

Abstract A manufactured aero-engine blade is commonly inspected in sections, and its geometric errors are evaluated from the sectional inspection data points. To maintain consistency in evaluating the geometric errors, in particular, the position and twist errors of the stacked blade sections, reconstruction of valid sectional airfoil profiles from the measurement points is preferred. Considering that inspection data points are subject to measurement uncertainty, profile reconstruction via approximation-based curve fitting, rather than interpolation-based curve reconstruction, is adopted in this work. The fitting error of the approximated airfoil profile is deemed equivalent to the measurement uncertainty in the inspection data points. Thus, according to a given measurement uncertainty value, a progressive curve fitting scheme is proposed to generate the airfoil profile that meets the measurement uncertainty constraint. A closed nonperiodic B-spline curve is utilized to model the reconstructed airfoil profile due to its versatility in closed curve approximation. Typical computational tests have been carried out to demonstrate the effectiveness of the proposed airfoil profile reconstruction method, which is in fact generic and can be equally applied to approximating other closed sectional profiles.

Keywords Airfoil inspection · Profile reconstruction · Measurement uncertainty · Closed curve approximation · B-spline

F. Khameneifar · H.-Y. Feng (✉)
Department of Mechanical Engineering, The University of British Columbia, Vancouver, BC, Canada V6T 1Z4
e-mail: feng@mech.ubc.ca

1 Introduction

Airfoil blades are key components in aero-engines. To maintain efficient energy conversion and survive the intense operating conditions, these blades need to be manufactured under extremely tight tolerances. Due to the unavoidable manufacturing errors, once a blade is produced, it must be precisely inspected in order to verify its conformance to the specified tolerances. In addition to being used as a means of acceptance or rejection of a manufactured part, correct representation of complete geometric error distribution on a manufactured blade also provides the fundamental data for improving the associated manufacturing operations.

The aero-engine blade tolerances are commonly specified and evaluated in sections. Some tolerances are effectively two-dimensional and section specific such as profile tolerance and airfoil dimensions, which are to be evaluated for each airfoil section individually. Other tolerances are three-dimensional, which are specified primarily to constrain the stacking of the airfoil sections with regards to the resulting position and twist errors. All of these tolerances and their associated geometric parameters are normally indicated on the engineering drawings for an airfoil blade. Typically, the associated geometric parameters include the leading edge point, trailing edge point, centroid of the airfoil profile, chord line, camber curve, maximum thickness, and orientation angle [1, 2]. The specific positions or values of these geometric parameters must be determined from the inspection data points in order to evaluate the related tolerances. Two challenges exist in this tolerance evaluation process. One is how to properly consider the measurement uncertainty present in the inspection data points. The other is how to determine the geometric parameters via a consistent approach across the various inspected airfoil sections for which the inspection data

points are collected under similar but different inspection conditions. The latter challenge is particularly important in evaluating three-dimensional position and twist tolerances of the blade from seemingly biased inspection data.

To successfully address both challenges stated above, it is proposed in this work to generate a continuous mathematical expression for the complete airfoil profile at each blade section from the discrete inspection data points. Due to the presence of measurement uncertainty, the inspection data points do not correspond to the actual points on the inspected blade surface exactly. As a result, the actual airfoil profile can never be precisely generated from the inspection data points. A valid approximation, however, can be generated according to the measurement uncertainty constraint. The measurement uncertainty-based approximation also provides the needed consistency in the systematic reconstruction of the individual airfoil profile at each blade section. With valid airfoil profiles consistently reconstructed at the inspected sections, the specified geometric tolerances on the blade, either two- or three-dimensional, are readily evaluated according to their definitions.

Existing studies attempted to evaluate the tolerances by determining the associated geometric parameters directly from the discrete inspection data points [2, 3] (without reconstructing the sectional airfoil profiles). Effectiveness of such an approach relies heavily on the consistency of the inspection process across the various airfoil sections, in particular in the evaluation of their position and twist errors. When the number and/or distribution of the collected data points vary among the inspected blade sections, biased computational results are likely produced. In these existing studies, it is evident that the consistency requirement was ignored and simplification was made to the three-dimensional tolerance evaluation procedure, which is possibly due to the challenge in reconstructing valid airfoil profiles from the inspection data points.

This paper presents a new, measurement uncertainty based airfoil profile reconstruction method, targeting the consistency requirement in three-dimensional blade tolerance evaluation. The reconstructed airfoil profile must be considered a feasible solution according to the measurement uncertainty constraint. A progressive curve fitting scheme is devised to reconstruct the airfoil profile that satisfies the imposed feasibility condition. A closed nonperiodic B-spline curve is used to represent the reconstructed airfoil profile due to its versatility in closed curve approximation. To ensure consistency, the reconstructed airfoil profile is to be generated without user input. As a result, a fully automatic closed B-spline curve approximation algorithm has been developed in this work, which improves on existing B-spline curve approximation methods. In the next section, the proposed criteria for airfoil profile reconstruction under the measurement uncertainty are described. Section 3 provides an overview on the existing B-spline curve approximation methods. Section 4 presents the proposed airfoil profile reconstruction method including the improvement made to the existing B-spline curve approximation methods. Section 5 illustrates some typical computational tests relevant to airfoil profile reconstruction, and Section 6 concludes the paper.

2 Criteria for airfoil profile reconstruction

A set of measured data points $\mathbf{Q}_i$ ($i=0$ to m) containing a known level of uncertainty is given. The known measurement uncertainty U is the expanded uncertainty, which defines an interval about the measurement result within which the actual value of the measurand should lie. The probability distribution in this interval is equivalent to the normal (Gaussian) distribution as shown in Fig. 1. An interval of $\pm 3\sigma$ (σ being the standard deviation of the normal distribution) is employed in the figure, which means that the actual value would lie within the uncertainty interval of the measured point with a 99.74 % probability [4].

Since planar coordinates are measured, the uncertainty interval for each measured data point can be considered as a circle centered on the measured point, with the diameter equal to the measurement uncertainty U. Figure 2 shows a series of measured data points on a plane along with their uncertainty intervals. According to the fact that the actual point corresponding to each measured point could lie anywhere inside the measurement uncertainty circle, a curve passing through all the circles is considered as a feasible approximation of the actual profile. Since the curve approximates the measured data points (by not passing through them), there exists a deviation e_i (a Euclidean distance) between the ith measured point and the approximated curve, namely the ith fitted residual. A quantity comparable to the expanded uncertainty U can then be derived from the fitted residuals to assess the feasibility of the approximated curve. More specifically, the standard deviation σ_r estimated as the root mean square (RMS) of the fitted residuals is to be multiplied by 6 and compared against U. The feasibility condition is then mathematically formulated as:

$$6\sigma_r \le U \tag{1}$$

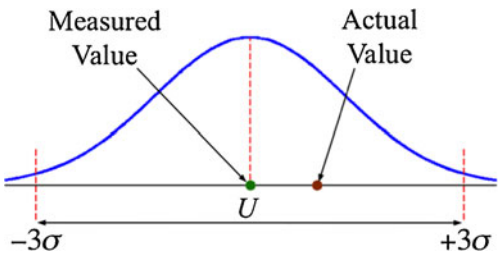

Fig. 1 Expanded uncertainty interval of $\pm 3\sigma$

There exist many curves that satisfy the above feasibility condition as shown in Fig. 2. In order to better approximate the actual airfoil profile, an additional criterion is introduced. This criterion is derived from the fact that the ideal CAD profile is smooth and without any redundant undulation. In order to establish the smoothest possible profile under the feasibility condition, the involved computation should not introduce unjustified undulation to the approximated curve. Hence, a feasible curve with minimum undulation is to be selected to best approximate the actual airfoil profile. For a composite polynomial curve of a fixed degree, a smaller number of segments would result in less undulation. Therefore, a progressive curve-fitting scheme is devised in this work to determine the feasible solution curve that employs the minimum number of segments. In this scheme, the algorithm starts with the smallest possible number of curve segments and then progressively increases the number of segments until the resulting curve satisfies the feasibility condition. The feasible curve with the minimum number of segments also has the benefit of data storage reduction and improved computational efficiency.

3 Curve approximation using B-splines

A B-spline curve $\mathbf{C}(u)$ of order p (degree $p-1$) is commonly expressed as:

$$\mathbf{C}(u) = \sum_{j=0}^{n} N_{j,p}(u)\mathbf{P}_j \qquad u \in [0,1] \tag{2}$$

where $\mathbf{P}_j$ are the control points and $N_{j,p}(u)$ are the B-spline basis functions of order p defined over the knot vector $\mathbf{U}=[u_0,u_1,\ldots,u_{n+p-1},u_{n+p}]$ [5–7]. The knot vector $\mathbf{U}$ consists of nondecreasing real-value knots. It is commonly desirable to use nonperiodic knots, which generate nonperiodic B-spline curves. The first and last p knots in a nonperiodic knot vector are duplicated. This makes the B-spline curve pass through the first and last control points and tangent to the first and last segments of the control polygon at the curve end points.

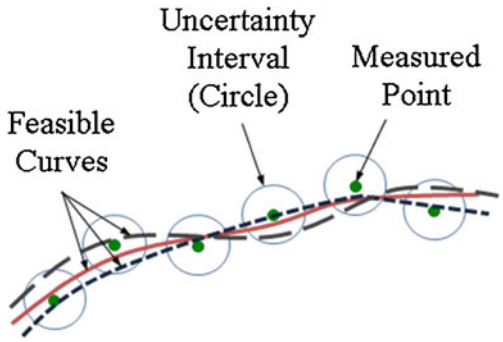

Fig. 2 Feasible approximated curves satisfying the uncertainty criterion

In order to fit a B-spline curve to a given set of points, some researchers have tried to solve this as a global nonlinear optimization problem by treating the parameter value at each data point, the number and location of the control points, and the knot vector as unknowns. Optimization schemes have been proposed, which start with an initial B-spline curve called the active curve [8–11]. The developed optimization algorithms will converge properly only if an appropriate active curve is specified. The active curve needs to be sufficiently close to the target curve shape and defined by an appropriate number of control points. Therefore, there still remain many challenges in the global nonlinear optimization approach and it is far from being fully automatic.

Instead of solving the global nonlinear optimization problem, a widely used method to approximate a B-spline curve from data points is via least-squares curve fitting. This approach involves three steps. First, the parameter value $\overline{u}_i$ for each data points $\mathbf{Q}_i$ is specified. This step is called parameterization. Second, a knot vector $\mathbf{U}$ is defined, corresponding to the parameter value $\overline{u}_i$, number of data points $m+1$, specified degree $p-1$, and number of control points $n+1$. This procedure is usually referred to as knot placement. The third step is least-squares minimization in which the location of each control points $\mathbf{P}_j$ is determined. The common practice is that the resulting curve would interpolate (pass through) the start and end data points, $\mathbf{Q}_0$ and $\mathbf{Q}_m$, and approximate (not pass through) the remaining points. Therefore, the locations of the first and last control points are respectively fixed at the start and end data points. In this case, in order to find the locations of the other control points, the following summation of least-squares deviations are minimized with respect to the $n-1$ variables, $\mathbf{P}_j$ ($j=1$ to $n-1$), where n is in general less than m:

$$\sum_{i=1}^{m-1} \left\| \mathbf{Q}_i - \mathbf{C}\left(\overline{u}_i\right) \right\|^2 \tag{3}$$

After differentiating Eq. (3) with respect to $\mathbf{P}_j$ and setting the resulting expressions equal to zero, the minimization problem is converted into one of solving a system of linear equations in the following form:

$$\left(\mathbf{N}^T\mathbf{N}\right)\mathbf{P} = \mathbf{R} \tag{4}$$

where $\mathbf{P}=(\mathbf{P}_1\ \mathbf{P}_2\ \cdots\ \mathbf{P}_{n-1})^{\mathrm{T}}$ and

$$\mathbf{N} = \begin{bmatrix} N_{1,p}(\overline{u}_1) & \cdots & N_{n-1,p}(\overline{u}_1) \\ \vdots & \ddots & \vdots \\ N_{1,p}(\overline{u}_{m-1}) & \cdots & N_{n-1,p}(\overline{u}_{m-1}) \end{bmatrix}_{(m-1)\times(n-1)} \tag{5}$$

$$\mathbf{R} = \mathbf{N}^{\mathrm{T}}\mathbf{Q} = \begin{bmatrix} N_{1,p}(\bar{u}_1)\mathbf{Q}_1 + \cdots + N_{1,p}(\bar{u}_{m-1})\mathbf{Q}_{m-1} \\ \vdots \\ N_{n-1,p}(\bar{u}_1)\mathbf{Q}_1 + \cdots + N_{n-1,p}(\bar{u}_{m-1})\mathbf{Q}_{m-1} \end{bmatrix}_{(n-1)\times 1} \tag{6}$$

Detailed derivation of the matrices above can be found in [7, 12]. Solving the derived system of linear equations requires a known knot vector. In order to compute the knot values, it is necessary to know the parameter value at each data point first. To compute the parameter value $\bar{u}_i$, many parameterization techniques have been proposed [13–16], among which the chord length method is the most widely used. Once the parameter values are computed, a knot vector is to be defined. De Boor [12] suggested a choice of internal knots to facilitate the least-squares approximation, which guarantees that every knot span contains at least one parameter value. When this condition is met, $(\mathbf{N}^{\mathrm{T}}\mathbf{N})$ in Eq. (4) is a positive definite matrix that makes the system of linear equations solvable by Gaussian elimination without pivoting.

It should be noted that the majority of the existing studies have been focusing on the approximation of open curves. The main difference between constructing an open curve and a closed curve lies in the clear indication of where the start point should be located. To construct a closed curve, there is no obvious location set for the start point with reference to the given point set. Therefore, there is a definite need to devise a systematic approach to select a suitable start point as a reference to parameterizing the data points. Parameterization can affect the shape of the fitted curve by altering the location of the solved control points. The method to select the start point must thus be sound in order to construct a curve with enhanced shape fidelity.

The above requirement for approximating closed nonperiodic B-spline curves over closed data point sets was raised by Piegl and Tiller [17]. They assumed that, in addition to data point positions, end derivatives were also available. End derivatives uniquely govern the locations of end control points. Thus, the computation of these control points was separated from the least-squares fitting procedure, where the rest of the control points were computed. This method suffers from the need of data point interpolation at the start and end control points. In addition, end derivative information is often not readily available for data point sets measured from closed profiles.

The curve approximation method devised in this work is in effect similar to that of Piegl and Tiller [17] in data point parameterization and knot placement. The main difference lies in its independence from the extra input information of end derivatives for selecting the start point. As a fully automatic method, the start point in this paper is selected based on the continuity constraints of a smooth closed B-spline curve. Compared with the existing methods, the set of parameters to be fitted in the proposed method is expanded to avoid any unnecessary interpolation of data points in generating the closed curve.

4 Profile reconstruction methodology

The airfoil profile reconstruction problem to be solved in this work can be formally defined as follows:

Given a set of discrete inspection data points $\mathbf{Q}_i$ (i=0 to m) and the associated measurement uncertainty, a closed nonperiodic B-spline curve of degree $p-1$ is to be computed to best fit the data point set such that it meets the feasibility condition and employs the smallest possible number of curve segments.

Figure 3 shows the flow chart of the overall profile reconstruction procedure. For a given number of curve segments, the procedure involves the following main steps:

1. Select an appropriate start point for constructing the curve.
2. Compute the parameter value for each data point starting from the selected start point.
3. Generate the knot vector using the computed parameter values at the data points as well as the number of control points so as to obtain the B-spline basis functions.

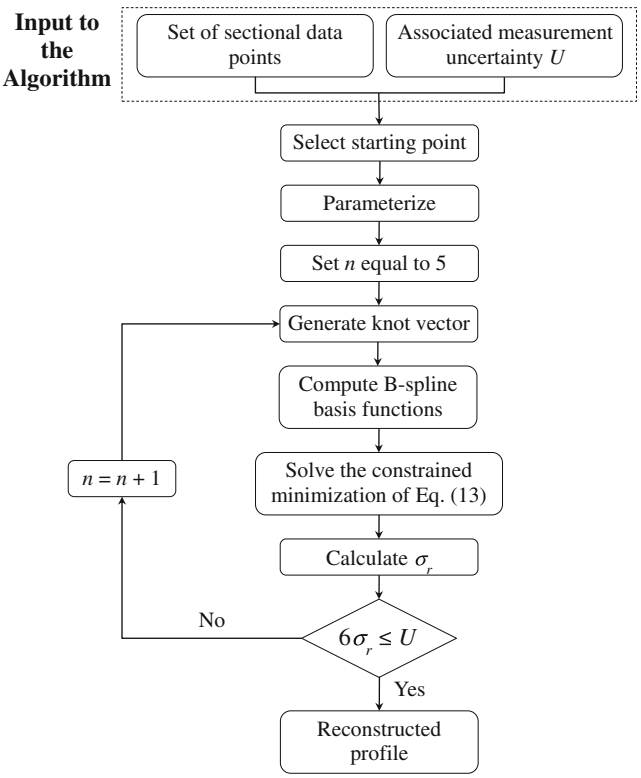

Fig. 3 Flow chart of the progressive profile reconstruction procedure

4. Determine the locations of the control points by solving the formulated least-squares minimization problem with the continuity constraints presented below.

The selection of an appropriate start point in step 1 is based on the continuity requirement for the best-fitted closed B-spline curve as applied to airfoil profile reconstruction. Airfoil blades are typically designed with curvature continuity since any curvature discontinuity would result in undesirable performance of the blades [18]. This means that, if an airfoil sectional profile is to be constructed as a piecewise polynomial curve, the resulting curve must provide at least C^2 continuity at the joint (knot) points of the involved curve segments. The continuity of a B-spline curve of degree $p-1$ is C^{p-2} at the knots. Thus, a cubic B-spline curve can provide the needed C^2 continuity. A higher degree would give higher continuity at the joints, but it may cause unwanted curve undulations. As a result, the cubic curve is employed to reconstruct the airfoil profile in this work. In order to obtain a smooth closed curve, continuity at the joint of the first and last curve segments (equivalent to the start as well as the end point) must be consistent with the continuity at all the other knots. Thus, for the closed cubic B-spline curve to be reconstructed, it needs to be C^2 continuous at the start and end points. This leads to the following continuity constraints on the associated control points:

$$\mathbf{P}_n = \mathbf{P}_0 \tag{7}$$

$$\mathbf{P}_n - \mathbf{P}_{n-1} = \mathbf{P}_1 - \mathbf{P}_0 \tag{8}$$

$$4(\mathbf{P}_0 - \mathbf{P}_{n-1}) = \mathbf{P}_2 - \mathbf{P}_{n-2} \tag{9}$$

Figure 4 shows a C^2 continuous closed cubic nonperiodic B-spline curve together with its control polygon. It should be noted that a nonperiodic B-spline curve passes through its first and last control points and its tangent vectors at the start and end points are, respectively, in the same direction as the first and last segments of the control polygon. Equation (7) requires that $\mathbf{P}_0$ and $\mathbf{P}_n$ should be placed at the same location (in order to form a closed curve). This constraint gives C^0 continuity at the start/end point, the joint of the first and last curve segments. Equation (8) gives C^1 continuity via equating the first derivatives of the closed curve at the joint, and Eq. (9) gives C^2 continuity by requiring the second derivatives at the start and end points to be the same.

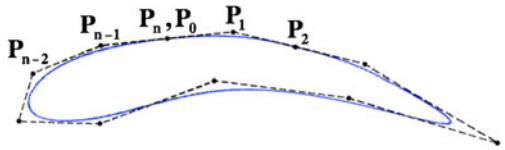

Fig. 4 A C^2 continuous closed cubic non-periodic B-spline curve (in *blue*) and its control polygon (in *black*)

From Eqs. (7) and (8), the set of control points $\{\mathbf{P}_{n-1}, \mathbf{P}_n = \mathbf{P}_0, \mathbf{P}_1\}$ should always be on a straight line, as can be seen in Fig. 4. This condition is to be used to select the start point. When a specific data point is designated as the starting point for parameterization (corresponding to the parameter value 0), it specifies a neighborhood for the potential location of the first and last control points. Due to the required C^2 continuity, the control polygon in this neighborhood should closely follow a straight line. Since the nonperiodic B-spline curve shares its tangents at the start/end point with the direction of both the first and last segments of the control polygon, the condition of the control polygon being close to a straight line in the start point neighborhood means that the curve will be geometrically flat around the start point. Therefore, the start point is to be selected as the point with minimum curvature variance along the airfoil profile.

In step 2, the popular chord length method [6, 7] is adopted to compute the parameter value for each data point:

$$\bar{u}_0 = 0, \quad \bar{u}_i = \bar{u}_{i-1} + \frac{|\mathbf{Q}_i - \mathbf{Q}_{i-1}|}{d}, \quad \bar{u}_m = 1 \tag{10}$$

where

$$d = \sum_{i=1}^{m} |\mathbf{Q}_i - \mathbf{Q}_{i-1}| \tag{11}$$

To generate the knot vector in step 3, the knot placement method by De Boor [12] is utilized in this work. For a nonperiodic B-spline curve of degree $p-1$ with $n+1$ control points, a knot vector of $n+p+1$ knot values must be defined. Since the first and last knots are duplicated p times, there are $n-p+2$ internal knot spans. While $u_0 = \ldots = u_{p-1} = 0, u_{n+1} = \ldots = u_{n+p} = 1$, the internal knots u_{p+j} are defined by:

$$\begin{aligned} u_{p+j} &= (1-\alpha)\bar{u}_{k-1} + \alpha\bar{u}_k \quad j = 0 \text{ to } n-p \\ k &= \text{Int}(jv) \\ v &= \frac{m+1}{n-p+2} \\ \alpha &= jv - k \end{aligned} \tag{12}$$

In step 4, the least-squares minimization problem is solved. One unique feature of the proposed method lies in avoiding any unnecessary interpolation of the data points. In particular,

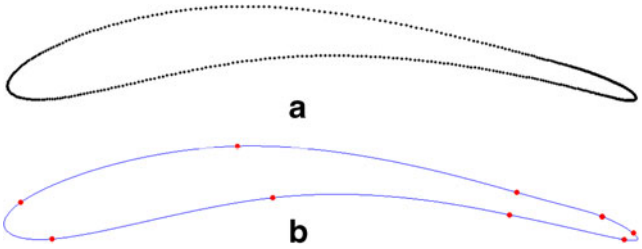

Fig. 5 **a** Ideal sampled points and **b** reconstructed profile of nine segments (in *blue*) along with its knot points (in *red*)

existing methods that interpolate the selected start/end data points are in effect inconsistent with the requirement that an approximated curve should not pass through any data point. Thus, in this work, the first and last control points are computed in the same way as all the other control points according to the imposed constraints of C^2 continuity. More specifically, the following objective function, in comparison with Eq. (3), is to be minimized with the constraints of Eqs. (7), (8), and (9) in order to solve for the complete control point set ($\mathbf{P}_0\ \mathbf{P}_1\ \mathbf{P}_2\ \cdots\ \mathbf{P}_{n-1}\ \mathbf{P}_n$) for the construction of a C^2 continuous closed B-spline curve:

$$\sum_{i=0}^{m} \left\| \mathbf{Q}_i - \mathbf{C}\left(\overline{u}_i\right) \right\|^2 \tag{13}$$

Once the control points are computed, the B-spline curve that approximates all the data points is obtained. The minimum possible number of control points to construct a closed cubic B-spline curve of C^2 continuity is 6. This means that at least three curve segments are needed to construct such a piecewise composite curve. Because of this, the progressive profile reconstruction algorithm proposed in this work starts with a curve composed of three segments (six control points). The resulting fitted curve is then checked against the feasibility condition of Eq. (1). If the feasibility condition is not met, one more curve segment (control point) is added and a new curve is fitted. This iteration continues until the feasibility condition is satisfied.

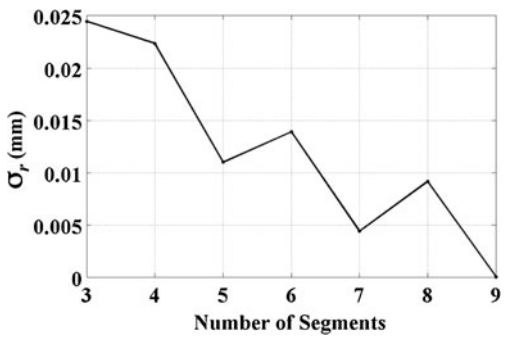

Fig. 6 RMS of the fitted residuals versus number of segments employed in the approximated curve (ideal sampled points)

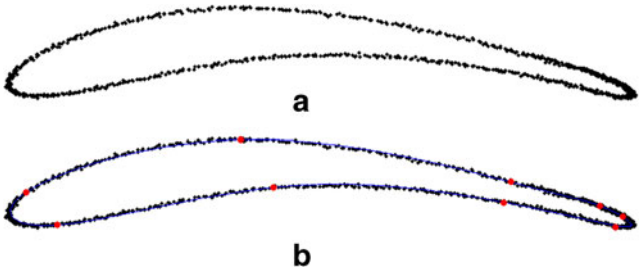

Fig. 7 **a** Noisy points with uncertainty and **b** reconstructed profile of nine segments (in *blue*) along with its knot points (in *red*)

5 Results and discussion

The proposed progressive profile reconstruction algorithm has been implemented and its effectiveness evaluated using many synthesized test data sets. Using synthesized data sets allows straightforward evaluation of the computed results against reference values in the test data sets.

5.1 Ideal data sets sampled from theoretical profiles

The first series of tests to assess the performance of the proposed algorithm are to validate the presented least-squares formulation with the continuity constraints in approximating closed curves. To perform this analysis, a theoretical B-spline curve is sampled into a sequence of 1,000 points. Then, the minimization problem is solved. Least squares, being a maximum likelihood estimator [19], would give the best approximate of the theoretical profile if the formulated mathematical expression for the curve fitting is correct. Hence, the minimum number of curve segments required, so that the fitted curve corresponds best to its theoretical solution, is expected to be exactly the same as the number of curve segments in the theoretical curve. Figure 5a shows the points sampled from a cubic closed nonperiodic B-spline curve composed of nine segments and joined with C^2 continuity, which resembles the shape of an airfoil profile. Since the minimum number of segments required to construct a C^2 continuous cubic closed nonperiodic B-spline curve is 3, the algorithm starts fitting the curve with three segments. Then,

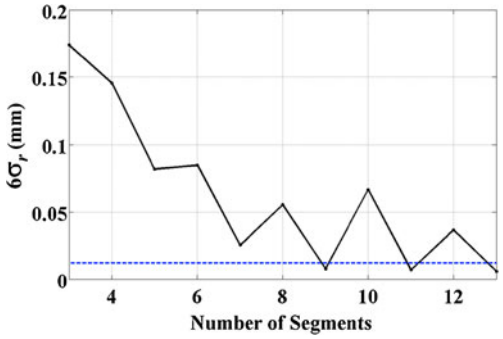

Fig. 8 $6\sigma_r$ versus number of segments in the approximated curve (*dashed line* indicating $U=12$ μm)

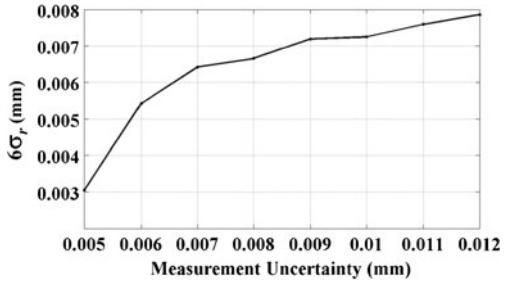

Fig. 9 Variation of $6\sigma_r$ (for approximated curves employing minimum number of segments) with different uncertainty intervals

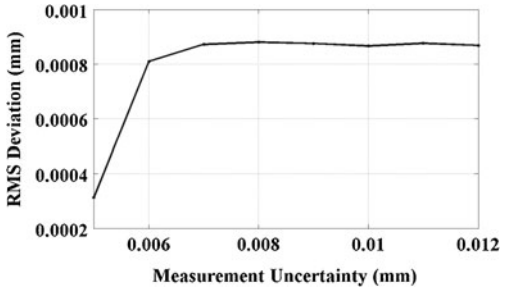

Fig. 10 RMS deviations between the approximated and theoretical profiles under different uncertainty intervals

the number of segments is increased incrementally. The RMS value of the fitted residuals of the approximated curve decreases with an increase in the number of curve segments until it drops to a value close to zero for nine curve segments. The fitted B-spline curve with nine segments shown in Fig. 5b corresponds very well to the original theoretical curve. The plot in Fig. 6 presents the RMS value of the fitted residuals, σ_r, of the approximated curve versus different number of curve segments employed in the approximated curve, from three to nine segments. The RMS value for the nine-segment curve is 3.6×10^{-5}mm, which indicates that the obtained solution reliably represents the original theoretical curve.

5.2 Synthesized noisy data sets

The previous set of 1,000 points is ideal and sampled from a theoretical curve. However, in practice, measured data points would contain measurement noise. As mentioned earlier, the input to the proposed algorithm is a data point set together with a known expanded measurement uncertainty interval. Reliable estimation of measurement uncertainty is difficult and varies with the measurement task being performed [20]. Savio and De Chiffre [21] developed a task-specific modular artifact to estimate measurement uncertainty in the inspection data of turbine blades. According to their reported results, the estimated measurement uncertainty is around 5–10 μm. In the present work, comparable Gaussian deviates are superimposed onto the ideal points shown in Fig. 5a in order to emulate noisy inspection data points characterized by different expanded measurement uncertainty intervals, ranging from 5 to 12 μm. Figure 7a shows a typical set of 1,000 points characterized with an expanded uncertainty interval of 12 μm.

As stated previously, one important feature of least-squares fitting is that normal (Gaussian) deviations in the fitted data will be dealt with automatically since least-squares is a maximum likelihood estimator. It is thus expected that the proposed progressive curve fitting on the noisy data set would end up with exactly the same number of curve segments as that for the ideal sampled points; i.e., nine segments. The computed results have shown that a feasible reconstructed profile from the noisy point set of Fig. 7a requires a minimum of nine curve segments as shown in Fig. 7b. Figure 8 illustrates how the RMS value of the fitted residuals, σ_r, decreases with increasing number of curve segments, starting from three segments. It can be seen that when nine curve segments are employed, the feasibility condition of $6\sigma_r \leq U$ is met. The dashed line in the figure, which corresponds to the termination criterion of the proposed algorithm, is set as the measurement uncertainty of the point set.

The RMS value of the fitted residuals is in effect equivalent to the standard deviation of normally distributed fitted residuals. Thus, once the $6\sigma_r$ value becomes less than the measurement uncertainty of 12 μm for the point set, the fitted B-spline curve is considered to lie within the uncertainty interval, making it a feasible solution. At the same time, the generated airfoil profile is characterized by minimum undulation since it contains the minimum possible number of curve segments to satisfy the desired shape fidelity. Another advantage of the feasible curve solution employing the least number of segments is that the constructed B-spline curve will be the simplest possible in formulation, as it employs the least number of defining knots and control points. Such simplicity makes it more computationally efficient to solve for the B-spline curve.

It should also be noted that, in practice, RMS of the fitted residuals is a more useful measure of closeness of the fitted curve to the input noisy points than other measures such as

Table 1 Minimum number of segments to reconstruct a feasible profile from point sets with different uncertainty values

Expanded uncertainty U (μm)	5	6	7	8	9	10	11	12
Minimum number of segments required	13	11/9	9	9	9	9	9	9

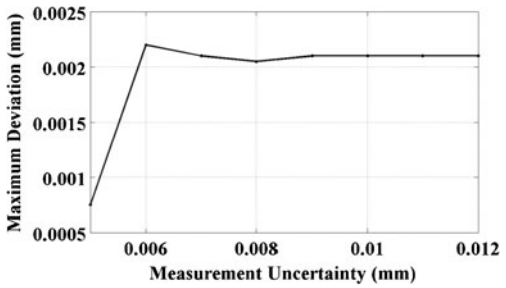

Fig. 11 Maximum deviations between the approximated and theoretical profiles under different uncertainty intervals

maximum deviation. This is because the RMS measure is much less sensitive to potential outliers in the point set. The maximum fitted residual of an approximated profile is likely to exceed the uncertainty interval, while the evaluated RMS of the fitted residuals would match the standard deviation of the underlying measurement uncertainty. Since the exceeded maximum fitted residual is often a result for noisy point sets, using the maximum deviation measure to confirm the feasibility condition of the fitted curve is likely to result in an incorrect minimum number of required curve segments.

Table 1 lists the minimum number of curve segments required to construct a feasible profile from point sets characterized with different uncertainty values. It can be seen that reducing the uncertainty in a point set tends to increase the number of curve segments required to form a feasible profile solution. When $U=6$ μm, close to half of the associated synthesized point sets require nine segments and the other half require 11 segments. When U is reduced further to 5 μm, 13 segments are needed. For the curves composed of the minimum possible segments corresponding to each uncertainty value as listed in Table 1, Fig. 9 shows the variation of $6\sigma_r$ (6×RMS of the fitted residuals) with the measurement uncertainty. As expected, the trend of variation of the RMS value is ascending with an increase in measurement uncertainty.

In Fig. 9, the RMS value of the fitted residuals is seen to grow at a reducing rate with measurement uncertainty. The significance of this reducing rate of growth can be illustrated by examining the degree of resemblance between the reconstructed profile under the imposed uncertainty and the theoretical reference profile. To examine this, both the RMS and maximum deviations of the reconstructed profile from the theoretical profile are adopted as measures of closeness. Variations of the RMS and maximum deviations with measurement uncertainty are shown in Figs. 10 and 11, respectively. As shown in these two figures, deviations between the approximated and theoretical profiles are not continuously growing with increasing measurement uncertainty in the point set. For interpolation-based reconstructed profiles, the general trend of such deviation plots would be ascending, which is due to the fact that the difference between the reconstructed and actual profiles increases as a result of the increased uncertainty. Conversely, for approximation-based reconstructed profiles using the proposed progressive algorithm, although the probability to accurately approximate the noisy data sets by the reconstructed profile still reduces with increased uncertainty, the reconstructed profile composed of the minimum possible number of segments for minimum curve undulation, is still faithful to the shape of the actual profile. This is confirmed by the implementation results of the proposed algorithm shown in Figs. 10 and 11 that the profiles have been reconstructed with similar degree of closeness to the actual profile even with increased measurement uncertainty values. The seemingly steady RMS and maximum deviations shown in the figures clearly indicate that the reconstructed profiles closely represent the actual profiles and are robust to the uncertainty in the input point sets.

6 Conclusions

A progressive curve fitting algorithm to reconstruct an airfoil profile from a given inspection data point set with a known measurement uncertainty has been presented in this work and is based on two criteria. The first criterion states that a constructed profile is considered a feasible solution if six times the standard deviation of the fitted residuals is less than the measurement uncertainty value. This means that the approximated curve would be within the expanded uncertainty intervals for the vast majority of the input points. Since numerous reconstructed curves can satisfy this criterion, the second criterion requires the curve to be of minimum undulation in order to be consistent with the general shape of an airfoil profile. The minimum undulation criterion in effect requires the curve to be constructed using the minimum possible number of curve segments. This will also bring the benefit of data reduction as a parametric curve with fewer segments results in fewer knots and control points. The implementation results have demonstrated the effectiveness of the proposed method. With the airfoil profile reliably reconstructed from a set of inspection data points, it can then be used to evaluate the stacking errors of airfoil sections in an airfoil blade. Relevant research work is underway and will be reported in the future.

Acknowledgments This research has been supported by Natural Sciences and Engineering Research Council of Canada (NSERC) under the CANRIMT Strategic Network Grant.

References

1. Pahk HJ, Ahn WJ (1996) Precision inspection system for aircraft parts having very thin features based on CAD/CAI integration. Int J Adv Manuf Technol 12:442–449
2. Hsu TH, Lai JY, Ueng WD (2006) On the development of airfoil section inspection and analysis technique. Int J Adv Manuf Technol 30:129–140
3. Chen L, Li B, Jiang Z, Ding J, Zhang F (2010) Parameter extraction of featured section in turbine blade inspection. In: Proceedings of the 2010 I.E. International Conference on Automation and Logistics, pp 501–505
4. Weckenmann A, Knauer M, Killmaier T (2001) Uncertainty of coordinate measurements on sheet-metal parts in the automotive industry. J Mater Process Technol 115:9–13
5. Farin GE (1992) Curves and surfaces for computer aided geometric design—a practical guide. Academic, New York
6. Hoschek J, Lasser D (1993) Fundamentals of computer-aided geometric design. Taylor & Francis, London
7. Piegl LA, Tiller W (1997) The NURBS book. Springer, New York

8. Pottmann H, Leopoldseder S, Hofer M (2002) Approximation with active B-spline curves and surfaces. In: Proceedings of the 10th Pacific Conference on Computer Graphics and Applications
9. Yang HP, Wang W, Sun JG (2004) Control point adjustment for B-spline curve approximation. Comput Aided Des 36:639–652
10. Wang W, Pottmann H, Liu Y (2006) Fitting B-spline curves to point clouds by curvature-based squared distance minimization. ACM Trans Graph 25:214–238
11. Liu Y, Pottmann H, Wang W (2006) Constrained 3D shape reconstruction using a combination of surface fitting and registration. Comput Aided Des 38:572–583
12. De Boor C (1978) A practical guide to splines. Springer, Berlin
13. Hartley PJ, Judd CJ (1980) Parameterization and shape of B-spline curves for CAD. Comput Aided Des 12:235–238
14. Hoschek J (1988) Intrinsic parameterization for approximation. Computer Aided Geom D 5:27–31
15. Cohen E, O'dell CL (1989) A data dependent parameterization for spline approximation. Mathematical methods in computer aided geometric design. Academic, San Diego, pp 155–166
16. Ma W, Kruth JP (1995) Parameterization of randomly measured points for least squares fitting of B-spline curves and surfaces. Comput Aided Des 27:663–675
17. Piegl LA, Tiller W (2000) Least-squares B-spline curve approximation with arbitrary end derivatives. Eng Comput 16:109–116
18. Koini GN, Sarakinos SS, Nikolos IK (2009) A software tool for parametric design of turbomachinery blades. Adv Eng Softw 40:41–51
19. Press WH, Teukolsky SA, Vetterling WT, Flannery BP (1992) Numerical recipes in C: the art of scientific computing. Cambridge University Press, New York
20. Wilhelm RG, Hocken R, Schwenke H (2001) Task specific uncertainty in coordinate measurement. CIRP Ann Manuf Technol 50:553–563
21. Savio E, De Chiffre L (2002) An artefact for traceable freeform measurements on coordinate measuring machines. Precis Eng 26:58–68